Application of Ripple Mapping to Visualize Slow Conduction Channels Within the Infarct-Related Left Ventricular Scar

Shahnaz Jamil-Copley, MRCP; Pasquale Vergara, MD, PhD; Corrado Carbucicchio, MD; Nick Linton, MRCP; Michael Koa-Wing, PhD, MRCP; Vishal Luther, MRCP; Darrel P. Francis, PhD; Nicholas S. Peters, PhD; David Wyn Davies, MD; Claudio Tondo, MD; Paolo Della Bella, MD; Prapa Kanagaratnam, PhD

Background—Ripple mapping (RM) displays each electrogram at its 3-dimensional coordinate as a bar changing in length according to its voltage–time relationship with a fiduciary reference. We applied RM to left ventricular ischemic scar for evidence of slow-conducting channels that may act as ventricular tachycardia (VT) substrate.

Methods and Results—CARTO-3© (Biosense Webster Inc, Diamond Bar, CA) maps in patient undergoing VT ablation were analyzed on an offline MatLab RM system. Scar was assessed for sequential movement of ripple bars, during sinus rhythm or pacing, which were distinct from surrounding tissue and termed RM conduction channels (RMCC). Conduction velocity was measured within RMCCs and compared with the healthy myocardium (>1.5 mV). In 21 maps, 77 RMCCs were identified. Conduction velocity in RMCCs was slower when compared with normal left ventricular myocardium (median, 54 [interquartile range, 40–86] versus 150 [interquartile range, 120–160] cm/s; $P<0.001$). All 7 sites meeting conventional criteria for diastolic pathways coincided with an RMCC. Seven patients had ablation colocating to all identified RMCCs with no VT recurrence during follow-up (median, 480 [interquartile range, 438–841] days). Fourteen patients had ≥1 RMCC with no ablation lesions. Five had recurrence during follow-up (median, 466 [interquartile range, 395–694] days). One of the 2 patients with no RMCC locations ablated had VT recurrence at 605 days post procedure. RMCCs were sensitive (100%; negative predictive value, 100%) for VT recurrence but the specificity (43%; positive predictive value, 35.7%) may be limited by blind alleys channels.

Conclusions—RM identifies slow conduction channels within ischemic scar and needs further prospective investigation to understand the role of RMCCs in determining the VT substrate. **(*Circ Arrhythm Electrophysiol*. 2015;8:76-86. DOI: 10.1161/CIRCEP.114.001827.)**

Key Words: myocardial ischemia ■ tachycardia, ventricular

The diastolic pathway of the re-entrant circuit of postinfarction ventricular tachycardia (VT) is formed through channels of slow-conducting viable myocardium within the scar.[1] These can be localized by activation or entrainment mapping during stable VT. Inconsistent inducibility and hemodynamic instability can limit this approach, and recurrence from VTs not induced at the index procedure is commonplace. Substrate modification has the benefit of being performed during sinus rhythm (SR) but requires the identification of all potential channels. Homogenization of the scar can be done by extensive ablation with an end point, such as noncapture at high pacing output.[2–9] This may obliterate all the channels, but the long-term consequences of such extensive damage on the already impaired ventricle are not known. Mapping and targeting only the slow conduction channels during SR would be a preferable option. Ablation of late potentials (LP) within the scar has been shown to be effective because it represents slow conduction traveling into the scar; however, the channels leading into scar may not connect back to normal myocardium to form a potential circuit.[9,10] Alternatively, modifying the bipolar voltage threshold used to define scar can reveal channels of higher voltage electrograms, within lower voltage scar, that bridge between normal myocardium.[11–13] The feasibility of such an approach has been proven, but the functional relevance of all such channels is not known. It is possible to check the local activation timing (LAT) of each electrogram for evidence of progressive activation, but the interoperator reproducibility of such a subjective approach has not been tested. These limitations highlight the technical problems in mapping scar using current technologies.

Received June 16, 2014; accepted November 13, 2014.

From the Department of Cardiac Electrophysiology, Hammersmith Hospital, Imperial College Healthcare Trust, London, United Kingdom (S.J.-C., N.L., M.K.-W., V.L., D.P.F., N.S.P., D.W.D., P.K.); Arrhythmology and Cardiac Electrophysiology Division, San Raffaele Hospital, University of Milan, Milan, Italy (P.V., P.D.B.); and Department of Arrhythmology and Electrophysiology, Centro Cardiologico Monzino, Milan, Italy (C.C., C.T.).

The Data Supplement is available at http://circep.ahajournals.org/lookup/suppl/doi:10.1161/CIRCEP.114.001827/-/DC1.

Correspondence to Prapa Kanagaratnam, PhD, Department of Cardiology, Hammersmith Hospital, Du Cane Rd, London, W12 0HS, United Kingdom. E-mail p.kanagaratnam@imperial.ac.uk

WHAT IS KNOWN

- Recurrence rates of ventricular tachycardia after ablation for scar-related ventricular tachycardia remain disappointingly high.
- Slow conduction channels within the ischemic scar have been proposed as the substrate for ventricular tachycardia to target for ablation but can be difficult to locate.

WHAT THE STUDY ADDS

- Ripple mapping is a novel method, which enables simultaneous visualization of voltage and activation data on the same 3-dimensional map. Each electrogram is represented as a dynamic bar with its base at the mapping site and height related to the bipolar electrogram voltage, which is time gated to a fiduciary reference.
- In infarct scar, ripple mapping revealed the sequential movement of the dynamic bars that preserved all of the low-amplitude deflections of fractionated electrograms, enabling the identification of slow conduction channels within the scar.
- It is hoped that the slow conduction channels revealed by ripple mapping may represent a more specific target for substrate-based ventricular tachycardia ablation approaches.

Ripple mapping (RM) is a novel visualization method, which displays each electrogram at its 3-dimensional (3D) coordinate on the cardiac shell as a dynamic bar moving out from the surface relative to a fiduciary time point. High-density point collection within a small area produces a ripple effect, with each bar changing according to the voltage change in a temporally accurate sequence, without the need to annotate a LAT. This enables simultaneous voltage and activation data on the same map displayed as sequential movement of dynamic bars preserving all of the low-amplitude deflections of fractionated electrograms.[14,15] We hypothesized that slow conduction channels can be visualized in the infarct scar using functional and structural data colocated on the same 3D geometry.

Methods

Patient Selection

Patients with ischemic scar were included. We reviewed endocardial electroanatomic maps (CARTO-3©; Biosense Webster Inc, Diamond Bar, CA) from 3 centers in Europe. RM requires high-density point collection within the scar; therefore, cases were reviewed and those identified with >150 left ventricular (LV) scar (<1.5 mV) points were selected arbitrarily for the study. All patients had provided written informed consent for the procedures.

Electrophysiology Procedure

Bipolar electrograms were recorded with a bandpass filter at 30 to 500 Hz using a 3.5-mm Navistar Thermocool catheter (Biosense Inc). A 6-F quadripolar catheter placed in the right ventricular apex was used for pacing, and a suitable surface ECG lead was selected as the fiduciary reference. LV access was gained via the retrograde transaortic approach or the trans-septal approach depending on operator preference. Electroanatomic maps were created using CARTO-3© during SR or right ventricular pacing. Acquired points were displayed according to local preference as bipolar voltage or LP maps. These have been described previously but briefly the bipolar voltage map was collected using a window of interest to include the surface QRS and the diastolic period up to the T wave. This map was displayed using standard scar settings with scar <0.5, scar border zone 0.5 to 1.5 mV, and healthy myocardium >1.5 mV. The LP map was created using a similar window of interest to the bipolar voltage map. The maximum peak or trough deflection of a surface QRS was chosen as the reference point and LPs, defined as low-amplitude (<1.5 mV) electrograms with a single or multiple components separated from the higher amplitude component of the local ventricular electrogram by ≥20 ms and recorded after the surface QRS end, were selected for the LAT. The LP LAT map was displayed by measuring the time from the reference electrogram to the end of the QRS with the latest inscription and using this for the minimum cutoff on the color scale. This ensured that the spectrum of colors displayed on the map represented activity occurring after the QRS (ie, LPs only).[10]

Anticoagulation with heparin was maintained throughout the procedures. VT was induced from the right ventricular apex, right ventricular outflow tract, or LV endocardial site using a standard VT stimulation protocol performed using an 8 beat drive train at 600 and 400 ms with ≤3 extra stimuli decremented down to 200 ms each until local refractoriness was encountered or VT was initiated.

If mappable VT was induced, conventional entrainment mapping was performed according to operator preference and the VT isthmus site(s) identified and tagged on the electroanatomic map. The VT isthmus was identified using conventional criteria, including entrainment with concealed fusion, stimulus to QRS <70% and >30% VT cycle length, a difference in the postpacing interval and tachycardia cycle length of 30 ms, and a stimulus to QRS and electrogram to QRS interval within 30 ms. Once the critical isthmus was identified, radiofrequency ablation was performed at the isthmus site, and on termination of the tachycardia a new point was tagged.[16,17] All sites associated with VT termination during ablation were also tagged on the map. After VT termination, additional substrate-based ablation was performed according to local protocols. Programmed ventricular stimulation was then repeated to test for inducibility of any ventricular arrhythmia.

Follow-Up

Patients were followed up routinely in the implantable cardioverter defibrillator clinic at their respective institutes or sooner if they experienced device therapy and data logged on appropriate device therapies.

Analysis of Electroanatomic Maps and Ripple Maps

All CARTO-3© maps underwent processing before analysis on RM to remove ablation and postablation points and any premature ventricular complexes, fused or paced beats during a SR map. For each map, the LV scar area and percentage were measured on the CARTO-3© system and documented including the number of scar points.

The cleaned maps of preablation sinus/paced activation were exported to an offline custom MatLab RM system. RMs were examined for conduction patterns within the scar, which was displayed on the 3D shell using standard baseline voltage settings for scar with an upper threshold of 1.5 mV (purple on RM) and a lower threshold of 0.5 mV (cyan blue on RM).

Identifying Conduction Channels

The RMs of the scar were played, and areas of sequential ripple bar propagation entering the scar from the scar border zone with progressive activation were identified. The threshold at which bars were visualized was gradually reduced to ensure that all small electrograms were displayed as bars. A minimum of 3 bars were necessary to identify such propagation with confirmation using LAT measurements.

Bars surrounding potential RM conduction channels (RMCC) were reviewed to confirm that the RMCC had activation distinct from the surrounding tissue.

To study the channel further, the surface bipolar voltage settings were adjusted by gradually reducing the upper threshold cutoff from 1.5 to 0.5 mV in 0.02 mV decrements. Below 0.5 mV, the difference in the upper and lower voltage thresholds was altered keeping a 0.02-mV difference until complete loss of any voltage gradient was achieved.

Once a channel was seen, the voltage settings were decreased to the minimum value, which identified the connections of the channel with the scar border (Figures 1 and 2; Movies I and II in the Data Supplement). If a channel of higher voltage (purple) was identified bounded by relative lower voltage (blue) on both sides, then this was considered a voltage gradient channel.

The presence of abnormal electrograms particularly in short channels with only a few ripple bars was also used to support the definition of RMCC. Abnormal electrograms included LPs, double potential (2 distinct bipolar potentials with peaks separated by an isoelectric portion with a return to baseline between the 2 potentials) and fractionated signals (low amplitude, high frequency, multicomponent signals of prolonged duration). These abnormal electrograms were sought along any identified channel as an indicator of slow conduction.

The points comprising the RMCCs were confirmed and drawn as design lines on the corresponding CARTO-3© maps using available online software. Ablation lesions were restored onto the CARTO-3© maps after creation of design lines representing RMCCs to examine the relationship between ablation lesions and identified channels.

The relationship between the location of entrainment data and VT termination during ablation, where available, was compared with the location of each RMCC.

Measuring Conduction Velocity

Conduction velocity (CV) was measured along each RMCC, excluding channels with significant bends. Channel length was measured point to point along the RMCC using standard CARTO software tools. As an example, in Figure 1D, the channel was measured along the bars colored yellow, blue, white, red, and green. The total length was the sum of the interpoint distances calculated using the CARTO measure distance function.

The majority of RMCCs consisted of complex multicomponent bipolar electrograms. Measurement of the LAT of such complex electrograms is challenging, and operator discretion is often required.[18,19] The adjacent panel in Figure 1D shows the bipolar electrogram at each point along the aforementioned channel. The time interval was the difference between the maximum amplitude

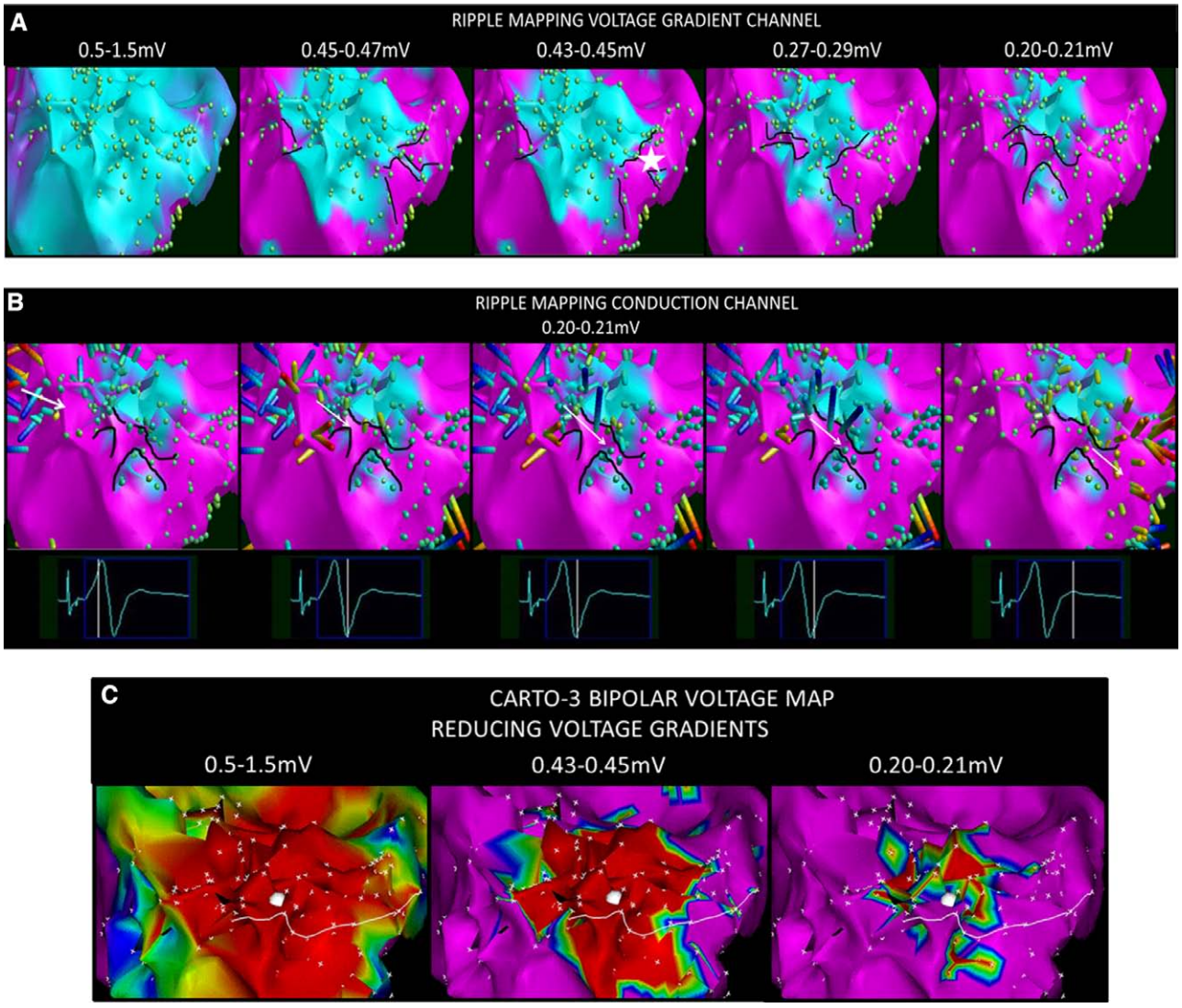

Figure 1. (*Continued*)

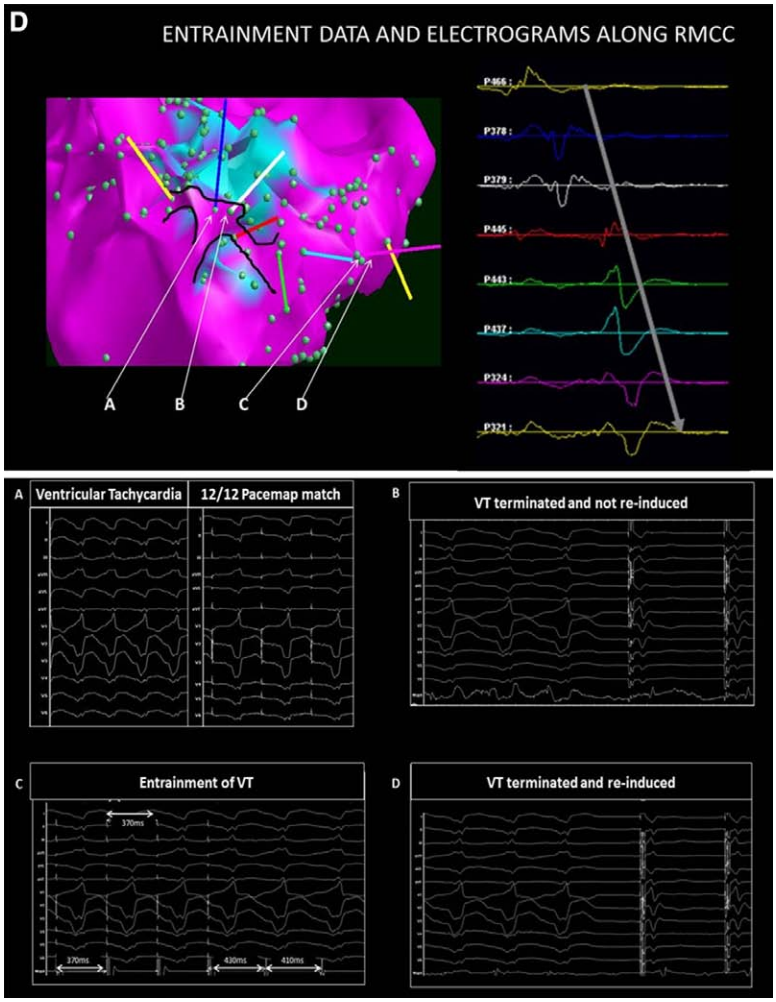

Figure 1. (Continued). Exposing a ripple mapping (RM) conduction channel 1. **A**, Left ventricular RM with standard scar settings allows appreciation of the scar border location (purple, healthy myocardium with a voltage of >1.5 mV; cyan blue, scar with a voltage <1.5 mV). The maximum ripple bar voltage is set at ±0.2 mV, which allows the visualization of electrograms at or above this value as dynamic ripple bars. The ripple bars have a graduated color spectrum, which enables the observer to appreciate the change in length even if the bar is viewed end-on. The color at the tip of the bar is green at zero-point and transitions to red when the voltage reaches the peak positive clipped value, or blue for peak negative clipped value. The surface voltage parameters are gradually reduced to allow visualization of a voltage gradient channel. After exposure of a voltage channel, the RM conduction through the channel is analyzed for contiguous activation of ripple bars confirming a RM conduction channels (RMCC), which is highlighted by the white arrow (**B**). The activation timing of the ripple bars in relation to the surface electrogram timing (as demonstrated by the white vertical line along the electrogram) can be seen at the **bottom** of **B** (Movie I in the Data Supplement). This demonstrates a sequential ripple bar activation channel from one end of scar to the other. The voltage gradient adjustments are displayed on the corresponding CARTO-3© map (**C**). **D**, The electrograms along the RMCC. At point A within the RMCC, there was a 12/12 pacemap of the clinical ventricular tachycardia (VT), and the adjacent point B was the successful site of VT termination during ablation with no inducibility. The white star (**A**) corresponds to termination of VT during ablation; however, this was re-inducible. Interestingly, point C was just outside the voltage criteria for the RMCC and was located in an area that would meet the conventional definition of scar border. Entrainment here revealed concealed fusion with a near-perfect return cycle length. Ablation at the adjacent point D led to VT termination but with reinduction. This suggests that points C and D may be in a wider part of the conduction channel as suggested by the third panel in **A** (0.43–0.45 mV), which fall into a different voltage gradient to the central portion of the channel containing points A and B (Movie I in the Data Supplement).

of the yellow and green electrograms that are encircled. CV of the RMCC was calculated as the RMCC length divided by the time interval between the first and last electrogram in the RMCC. RMCC conduction was compared with wavefronts in normal myocardium. Ripple bar propagation was analyzed in healthy myocardial regions (>1.5 mV); if linear activation (eg, from base to apex or vice versa) was visualized with a row of electrograms in the direction of propagation, then the length in a sample area was measured (distance between earliest and latest electrogram) along with the LAT of these electrograms to calculate the CV. Only maps with a map point density in normal myocardium of ≥0.5 per square centimeter were included in this analysis. This was not possible on all the maps because of insufficient point density in the normal myocardium in the direction of wavefront propagation.

Statistical Analysis

Parametric variables were tested using the independent Student 2-tail *t* test for statistical differences between sample groups. Nonparametric data was tested using the Mann–Whitney test for comparison of independent samples and the Wilcoxon signed-rank test for paired samples. Continuous parameteric data are expressed as mean±SD and nonparametric data as median (interquartile range [IQR]). Statistical analyses were performed using SPSS version 16.0

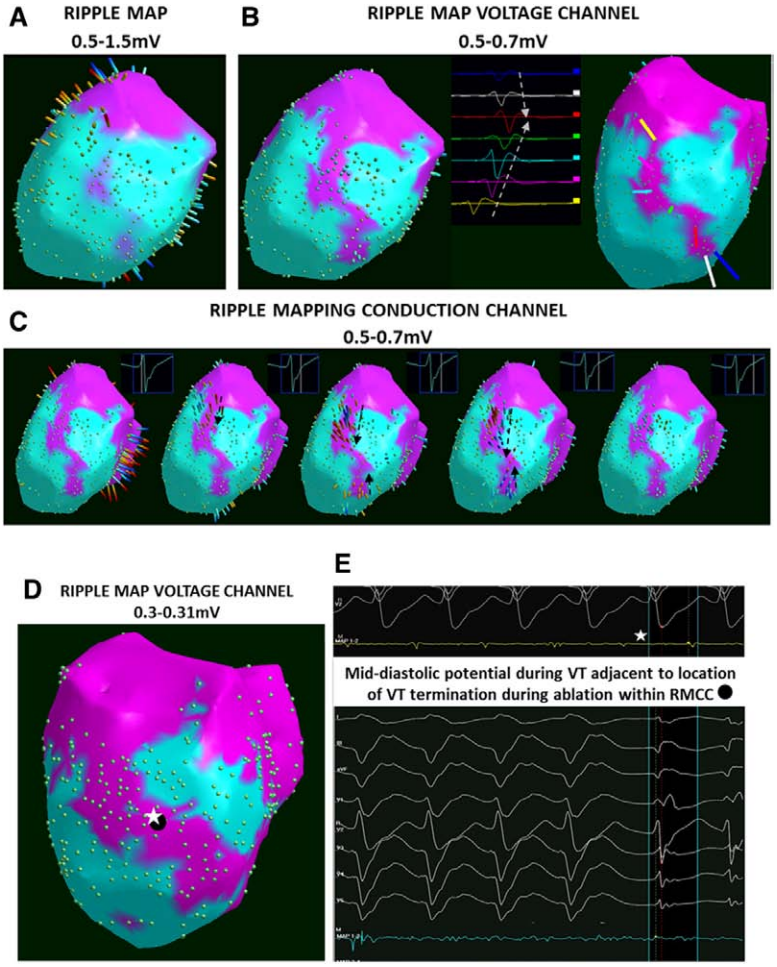

Figure 2. Exposing a ripple mapping conduction channel (RMCC) 2. A left ventricular RM with standard scar settings in **A** demonstrates the scar border location (purple, healthy myocardium >1.5 mV; cyan blue, scar with a voltage <1.5 mV). The maximum ripple bar voltage is set at ±0.45 mV, which allows the visualization of electrograms at or above this value as dynamic ripple bars. The ripple bars have a graduated color spectrum, which enables the observer to appreciate the change in length even if the bar is viewed end-on. The color at the tip of the bar is green at zero-point and transitions to red when the voltage reaches the peak positive clipped value, or blue for peak negative clipped value. As the surface scar voltage is reduced to 0.7 mV, a channel of higher voltage (purple) is visualized through scar (**B**). Bidirectional activation of the channel as displayed by the ripple bar propagation can be appreciated (the activation timing of the ripple bars in relation to the surface electrogram timing is shown in the **top right** of each panel; **C**). The colored bars along the channel in **B** allow a virtual display of the electrograms, which participate in the RMCC and correspond to the colored electrograms (in the same panel) confirming the chevron activation pattern of the channel as visualized on the ripple map. As the voltage is reduced further to 0.3 mV, the RMCC is visualized fully from one end of the myocardium across the scar to the other (**D**). **E**, The diastolic electrograms seen within this channel during ventricular tachycardia (VT; starred), which terminated during ablation at this location (black dot) (Movie II in the Data Supplement).

(IBM SPSS Statistics; IBM Corporation, Armonk, NY). A *P* value <0.05 was considered statistically significant.

Results

Study Population

Twenty-one consecutive patients identified with LV maps with >150 scar point were analyzed. All patients had an implantable defibrillator. Demographics are displayed in Table 1.

Preablation Mapping

The 21 maps analyzed were created during SR in 17 cases and during ventricular pacing in 4 cases. Median map density was 397 points (IQR, 322–573) with a scar area of 34% (IQR, 26–47) by standard scar bipolar voltage criteria of ≤1.5 mV (Table 2). The median number of scar points were 318 (IQR, 219–371) with a scar point density of 3.4 (IQR, 2.5–3.8) points/cm^2. In 3 patients, VT was not inducible at the start. In the remainder, a median of 2 VTs was induced. Scar distribution included inferior wall in 16 maps and anterior wall in 9 maps with septal involvement in 4; lateral involvement in 2; apical involvement in 16; and basal involvement in 15 maps using conventional bipolar scar setting of 0.5 to 1.5 mV. In 6 patients, conventional electrophysiological data were available including entrainment mapping and pace-mapping.

RM Analysis to Identify Conduction Channels

Figure 1 and Movie I in the Data Supplement illustrate the steps in identifying a RMCC. Movie I in the Data Supplement shows the RM being played with gradual reduction of both the maximum ripple bar voltage, which brings bars with low electrogram amplitude into view, as well as the bipolar scar voltage, which changes the color of the surface geometry, to assess for voltage channels. Toward the end of the adjustments, a clear activation of ripple bars is seen across the scar. Selection of a series of electrograms (shown in the window) along this RMCC confirms progressive activation. Figure 1A shows that by adjusting the bipolar voltage, it is possible to see different portions of this RMCC using the voltage gradient approach, but Figure 1B confirms that the Ripple Map displays a longer RMCC than can be appreciated by the voltage channel using a single voltage threshold. Figure 1C shows this voltage channel in a more conventional CARTO-3 format for illustrative purposes. Figure 1D shows electrograms along the entire RMCC which extend beyond the voltage channel. Conventional maneuvers confirm that electrograms along the entire RMCC meet diastolic pathway criteria.

Movie II in the Data Supplement shows another example of a RM being played with the maximum ripple bar voltage reduced to gradually view smaller electrograms while simultaneously reducing the surface scar bipolar voltage. A chevron of distinct activation is seen as this process is completed

Table 1. Patient Demographics

	Mean±SD	Range
Age, y	69±7	49–79
Sex (men), n (%)	21 (95)	…
Infarct scar location, n (%)		
Anterior	9 (43)	…
Inferior	16 (76)	…
Apical	16 (76)	…
Basal	15 (71)	…
Septal	4 (19)	…
Lateral	2 (9)	…
LV ejection fraction, %	28±6	15–38
Device, n (%)		
ICD	13 (62)	…
BiV-ICD	8 (38)	…
Revascularization, n (%)		
None	8 (38)	…
CABG	6 (29)	…
PCI	8 (38)	…

BiV-ICD indicates biventricular implantable cardioverter defibrillator; CABG, coronary artery bypass graft; LV, left ventricular; and PCI, percutaneous coronary intervention.

(Figure 2A and 2B). Figure 2C shows each step with activation entering scar from opposite directions indicating that the bar and voltage threshold needs to be reduced further after which the entire RMCC, bridging healthy tissue, is visible. This technique allows the identification of the lowest bipolar amplitude regions with conduction properties. Figure 2D and 2E shows the termination site relative to the RMCC.

Movies III and IV show further examples of RMCC, which were also not as distinct on the RM alone because of point density but in the presence of abnormal electrograms support the view that these were RMCCs. These movies in the Data Supplement demonstrate channels of sequentially activating ripple bars containing abnormal electrograms (fractionation is seen as bars which continually go up and down throughout the channel activation, double potentials are seen as ripple bas going up and down twice within the same activation cycle, and LPs seen as late ripple bar activity after the inscription of the latest surface QRS-see top right of the screen) of relatively higher voltage when compared with surrounding electrograms (demonstrated by larger ripple bars immediately surrounded by small ripple bars).

Table 2. Mapping and Ablation Data

	Median	IQR
Map density, n	397	322–573
Scar and SBZ area, cm^2	91	58–120
Total scar and SBZ, %	34	26–47
Carto points in scar and SBZ, n	318	219–371
Map scar point density, cm^{-1}	3.4	2.5–3.8
VTs induced, n	2	1–3

IQR indicates interquartile range; SBZ, scar border zone; and VT, ventricular tachycardia.

Twenty-one maps were analyzed. A total of 87 voltage channels were identified. Seventy-seven were confirmed as RMCCs. Thirty three were identified with the upper voltage cutoff between 0.5 and 1.5 mV; 15 within a range of 0.31 and 0.49 mV and 29 in ≤0.3 mV window. The mean upper (range, 0.5–1.5 mV) and lower (≤0.5 mV) cutoff values for identified channels were 0.72±0.21 and 0.3±0.12 mV, respectively.

RM data were validated using LAT measurements of a total of 377 electrograms (mean, 4.9±1.5 electrograms/RMCC). A percentage of 96 RMCCs were associated with abnormal electrograms including isolated LPs, fractionated signals, or double potentials (Movies in the Data Supplement). Twenty three of 77 (30%) channels formed a continuous tract from healthy myocardium (voltage criteria, ≥1.5 mV) through scar to healthy myocardium with evidence of electric propagation through the channel.

Normal myocardial CV measurement was possible in 9 patients. The median RMCC CV was 54 cm/s (IQR, 40–86) compared with 150 cm/s (IQR, 120–160) in the normal LV myocardium ($P<0.001$). The CV was slower moving from the scar border zone (1.5–0.5 mV) into the scar (<0.5 mV), but this was not significantly different (77 cm/s IQR, 39–92 versus 51 cm/s, IQR 41–70; $P=0.38$).

All 7 documented locations displaying entrainment with concealed fusion (n=2) or perfect pace matches (n=5) to induced/clinical VT coincided with an identified RMCC. The design line in Figure 1C shows the location of the RMCC superimposed on a standard CARTO bipolar voltage map. In this case, it is clear that point B was a better location for ablation than point D because this is a central narrow portion of the RMCC. In the case displayed in Figure 1D, ablation at the RMCC site with the lowest voltage (≈0.25 mV) successfully terminated tachycardia without reinducibility (Figure 1D, B); however, VT was also terminated during ablation at the higher voltage site along the RMCC (≈0.47 mV) but with reinduction (Figure 1D, D).

Postablation Analysis

In 4 patients, VT terminated during ablation. Termination sites correlated with RMCCs in 3 patients (Figures 1D and 2D). The point density around the termination site in the fourth patient was insufficient to identify any channels in this region.

Ablation lesions overlapped with all identified RMCCs in 7 patients. In these 7 patients, ablation lesions coincided with a total of 17 RMCCs (mean, 2.4±1; range, 1–4) with a median length of 25 mm (IQR, 22–34 mm) and CV of 48 cm/s (IQR, 28–70 cm/s). Figure 3 shows an example of colocation of ablation with all identified RMCCs.

In 14 patients, not all RMCC sites colocated with ablation lesions of whom 12 had >1 RMCC present. Figure 4 shows examples of RMCCs remnant after ablation.

Follow-Up

VT was noninducible after ablation in 14 (78%) of the 18 patients in whom it was previously inducible. Four (29%) of these patients had recurrence of VT during follow-up. VT was still inducible after ablation in 4 (22%) of 18 patients in whom

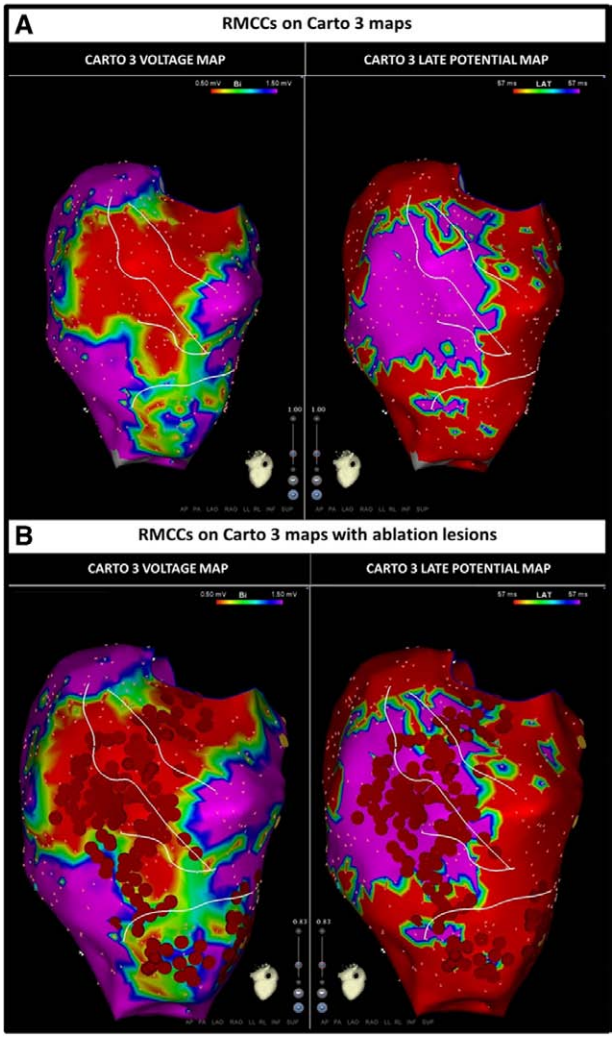

Figure 3. Ablation overlapping all ripple mapping conduction channels (RMCCs). CARTO-3© bipolar voltage map (0.5–1.5 mV) and corresponding late potential map (set at 57 ms) are displayed with design lines for the identified RMCCs (**A**). All RMCCs overlap areas with late potentials (**right**). Ablation lesions restored onto the map overlap all of the RMCCs (**B**). In this patient, ventricular tachycardia (VT) became noninducible after ablation having previously been inducible. There has been no recurrence of VT during a follow-up period of 429 days.

it was previously inducible. One (25%) of these patients had VT recurrence during follow-up (Figure 4). One patient died remote of their repeat ablation procedure because of severe heart failure with no evidence of VT recurrence on implantable cardioverter defibrillator interrogation.

Five of 21 patients had VT recurrence during a median group follow-up of 466 days (IQR, 395–694 days). There was no VT recurrence in patients (n=7) with all RMCC locations ablated during a median follow-up time of 480 days (IQR, 438–841 days). One of the 2 patients with no RMCC locations ablated had VT recurrence at 605 days post procedure.

In patients where ablation tags colocated to all RMCC sites, there was a negative predictive value of 100%, whereas a negative VT stimulation study post ablation had a negative predictive value of 76%. However, the presence of RMCCs without colocated ablation tags had a positive predictive value of 36%, and a positive VT stimulation study had a positive predictive value of 25%. The sensitivity and specificity of VT inducibility using the VT stimulation study post ablation was 20% and 81%, respectively, when compared with 100% and 45% for presence or absence of RMCC, respectively. Therefore, this limited series suggests that the presence of RMCCs may be more useful than VT stimulation for predicting VT recurrence after ablation.

Comparison of the baseline RMCC characteristics between patients with and without VT recurrence did not show a significant difference between the median length of the RMCC (23.7, IQR, 19–33.5 mm versus 32.6, IQR, 23–47 mm; P=0.32) or the CV (55, IQR, 36–77 cm/s versus 54, IQR, 44–87 cm/s; P=0.45).

Repeat Procedures

Three patients attended for repeat ablation procedures. Map scar point density, number of identified RMCCs, and the median scar area were not significantly different at the repeat procedure (Figure 5). RMCCs were identified at lower voltage gradients with slower CVs at the second procedure (median, 0.5 versus 0.32 mV; P=0.03 and 78 versus 69 cm/s; P=0.1, respectively).

Comparison of the bipolar voltage maps with RMCCs displayed as design lines from the index and repeat procedures for each patient revealed the absence of some of the initial RMCCs (which colocated with ablation lesions) at the repeat procedure. In addition, new RMCCs were often identified at the repeat procedure for each patient. Closer examination of the maps from the index and repeat procedures revealed a lack of sufficient points in the location of the RMCC sites at the index procedure or presence of new scar in these locations at the repeat procedure.

Discussion

This study describes the technique of visualizing slow conduction channels within the infarct scar. Using RM to display electric propagation and scar location on the same 3D geometry, it is possible to perform functional and anatomic mapping of the infarct scar during SR in a manner that is not possible with current mapping systems. RM is the only mapping system that allows the display of voltage and activation simultaneously preserving and displaying abnormal electrograms. This allows immediate appreciation of regions of slow conduction and sequential higher amplitude activation within scar with regions of discordant surrounding activity with minimal, if any, operator annotation.

Although this information can be gathered using current 3D mapping systems, it would involve adjustment of the voltage thresholds to highlight channels, followed by individual electrogram analysis with LAT assignment of complex low-amplitude electrogram morphologies, which would be repeated for all neighboring electrograms. We have demonstrated that voltage criteria alone display only a part of the entire activation channel; therefore, depending on the finding, the voltage threshold would then need to be readjusted and the process repeated until the entire activation channel was categorized. This would need to be repeated for each channel visualized.

An additional indirect advantage of RM is that it forces the operator to acquire more points because there is no data interpolation. As each point does not need annotation on

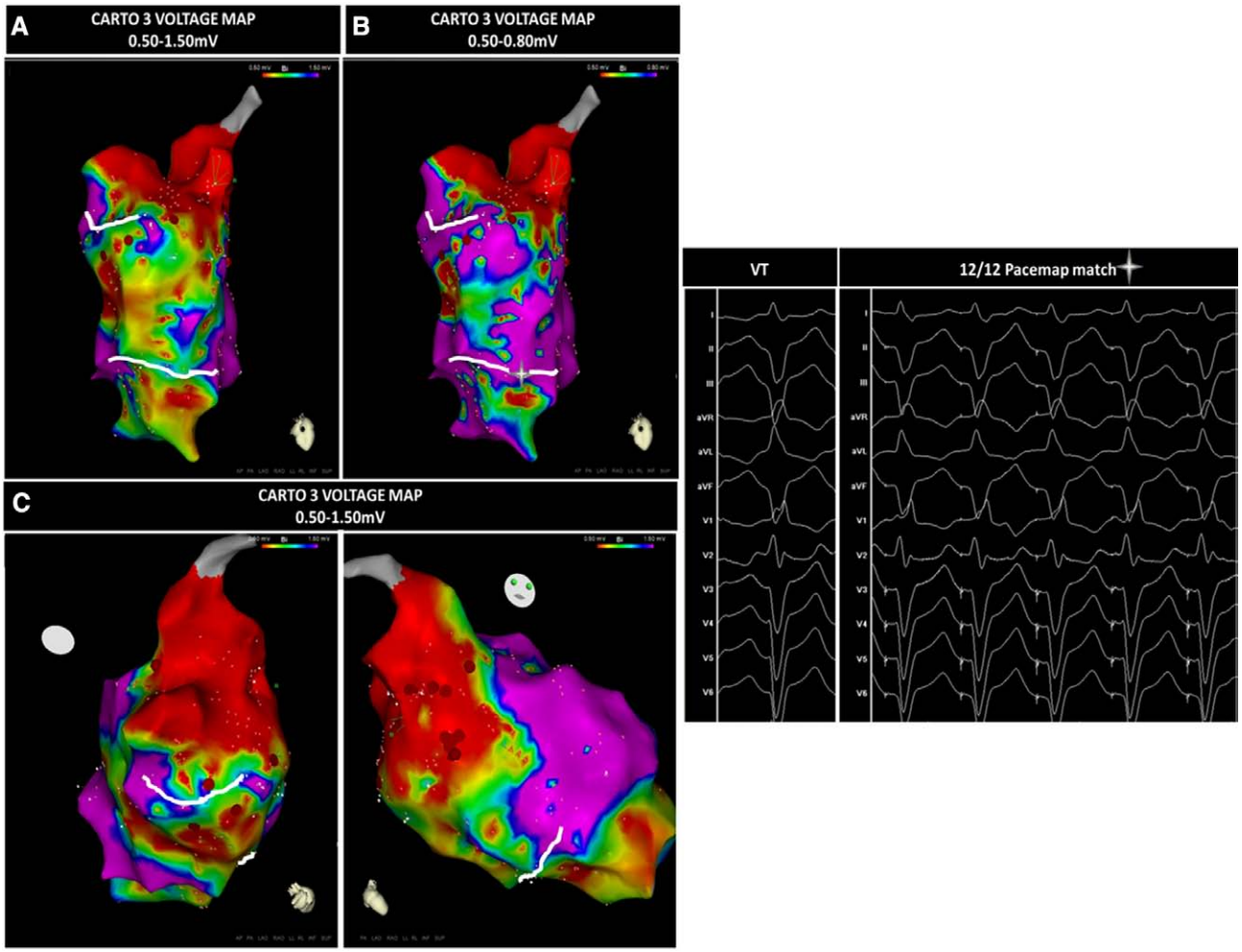

Figure 4. Presence of all ripple mapping conduction channels (RMCCs) post ablation. **A**, A CARTO-3© map at standard bipolar voltage settings (0.5–1.5 mV) and in **B** with a voltage gradient setting of 0.5 to 0.9 mV displaying the identified RMCCs. Design lines in white highlight the RMCCs. Retrospective review of the study revealed a 12/12 pacemap match for a nonclinical ventricular tachycardia (VT) when pacing was performed from the lower RMCC (starred). This patient had 7 morphologies of VT during the ablation procedure. The ablation strategy was to target the clinical VT, but 2 nonclinical VT morphologies that occurred frequently during the case were also ablated and the ablation lesions are shown. Only 1 RMCC was identified in the vicinity of the ablation lesions predominantly because of insufficient map point density at these locations. None of the ablation lesions colocated to the identified RMCCs. VT was noninducible post ablation having been previously inducible. The patient had recurrence of VT 605 days after ablation.

RM, operators do not need to be concerned about post-processing times. This, in turn, results in a more accurate diagnosis. We have previously shown that RM improves diagnostic speed and accuracy in atrial tachycardias, and we would expect the same to hold true for ventricular scar mapping.[15]

The study also demonstrates the concept of adjusting the threshold to define bipolar scar voltage using local propagation/activation rather than preassigned values, which are not patient specific. The RMCCs varied in length and conduction properties, with some traversing the entire scar and showing a chevron activation pattern with conduction entering the channel from both sides. At least 1 RMCC was identified in all patients although several were incomplete channels. This may be because of insufficient point collection, blind alleys, or components deep in the myocardium or epicardium. The presence of multiple RMCCs of variable lengths and conduction velocities in most patients illustrates the heterogeneous and complex scar architecture that can be exposed by RM.

Identifying channels using voltage criteria only requires the selection of set voltage thresholds. Studies have suggested that a bipolar voltage of <1.5 mV is appropriate for locating scar.[2,20] However, there are no criteria for subdividing this range further between functional tissue and infarcted tissue displaying far-field signals only. Pacing captures viable tissue but may not be specific at the high outputs needed in scar. Adjustment of voltage threshold will demonstrate channels, but without functional verification, this process is unlikely to be maximally advantageous because portions of a conducting channel can lie within different bipolar voltage gradient ranges (Figure 1; Movie I in the Data Supplement). Visualizing the entire conduction channel enables the operator to decide where the optimal site for ablation is compared with seeing part of the channel using voltage guidance only.

RMCC mapping also introduces the possibility of an end point for substrate ablation because the scar can be mapped after RMCC ablation to demonstrate block into the channel.

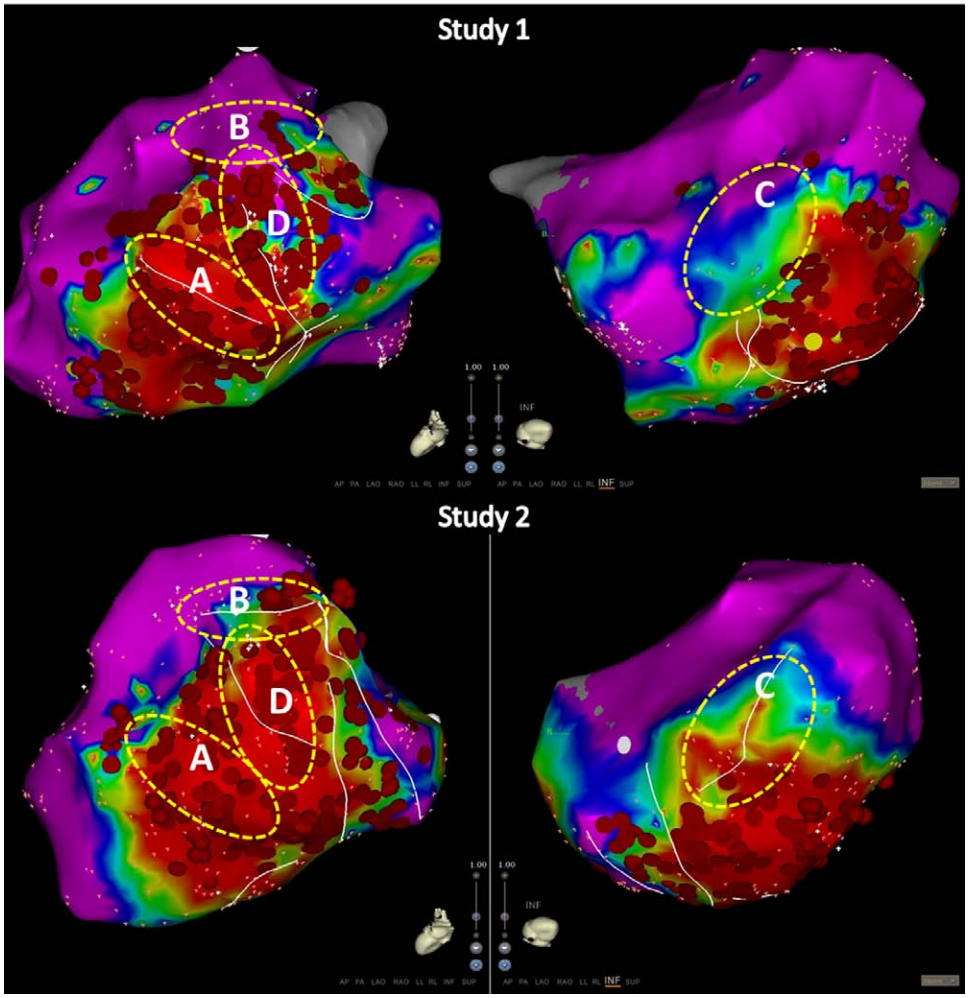

Figure 5. Initial and re-do ablation procedure. **Top**, A CARTO-3© bipolar voltage map from the initial procedure of a patient who attended for a repeat ablation 9 days later. Bipolar voltage settings are 0.5 to 1.5 mV. **Bottom**, The bipolar voltage map (same settings) from the repeat ablation. White design lines on the maps represent the location of ripple mapping conduction channels (RMCCs) from analysis of the ripple maps. The scar area is larger at the repeat procedure (**bottom**; 49 vs 68 cm2; map point density 8.4 vs 4.5). The map demonstrates evidence of a RMCC identified at the index procedure, which is not present at the repeat ablation and coincides with ablation at the index procedure (A). Two examples are also shown of RMCCs identified at the second procedure, which were not seen at the index ablation (B and C). This may be because of insufficient points in these regions at the index procedure or presence of new scar at the repeat procedure. Encircled in D is a RMCC identified and ablated at the first procedure with the continuation of the same channel identified at the second ablation. It is possible that this is the extent of the entire channel (from one scar border zone to another), which was not fully appreciated at the index procedure because of insufficient map point density. The presence of this RMCC despite ablation at the index procedure may reflect an epicardial circuit with insufficient ablation transmurality at the index procedure. AP indicates anteroposterior; INF, inferior; LAO, left ventricular outflow; LL, lateral; PA, posteroanterior; RAO, right ventricular outflow; and SUP, superior.

This can only be done in a prospective study with a clinical version of the software.

Entrainment studies suggest a complex architecture in ischemic scar with electric activity passing into adjacent and remote bystander sites, as well as traveling through the diastolic channel.[16,17] However, it is only possible to use these functional descriptions when mapping stable VT. In the current study, sites of 12/12 pace-matches and entrainment with concealed fusion with perfect return cycles colocated to RMCC sites providing supportive evidence that RMCCs have a functional role in VT. As this was a retrospective series, most RMCC regions did not have any pacing assessment. We would speculate that some of the channels identified do not have a role in providing substrate for VT and form blind alleys or bystander circuits during VT. We were not able to differentiate between these possible types of RMCCs, and a prospective series would be required to characterize the RMCCs further using pacing maneuvers.

Ventricular substrate ablation techniques attempt to locate and ablate the potential central isthmuses using scar location only (homogenization of scar), activation timing (LP ablation), or voltage gradients (bipolar voltage mapping) during SR using predefined scar voltages, which are based on arbitrarily set values extrapolated from endocardial data collected from anterior aneurysms and small sample sizes.[2–10,20] These methods have been used because there have been limited techniques for mapping the scar, and the current study provides indirect evidence that targeting the functionally relevant parts of the scar may prevent VT recurrence. The difficulty in quantitatively and objectively defining abnormal/LPs can limit

their reproducibility in studies using this as a basis for substrate ablation. LP maps restricted to sinus/paced rhythm diastolic potentials are likely to substantially underestimate the VT substrate. This is an another potential advantage of RM.

It is not known whether the extensive ablation used during scar homogenization, LP ablation, and scar voltage–based approaches also have a proarrhythmic effect when ablating in nonarrhythmogenic regions or a detrimental effect on long-term survival from reduced LV function. In the patients who had repeat studies, there was evidence of new RMCCs and larger scar areas, suggesting that these risks are theoretically possible.

Because this was a retrospective study, we chose to select studies with ≥150 LV scar points. This provided a sufficiently dense scar region for our analysis; however, gaps in data collection were evident, sometimes in crucial areas. We identified that maps collected using a fill threshold <5 mm to form coalescent geometry with electrogram data in the area of interest produced optimal RMs, which we would recommend for any prospective study. This may require further filling with points to highlight the intricacies of identified RMCCs (ie, blind alleys versus complete channels). Multielectrode mapping may facilitate this process.

On the basis of the current study, we would propose that RMCCs should include 4 of the following 5 features: (1) clear sequential movement of >5 dynamic bars entering the scar from the scar border zone with progressive LAT, (2) ripple bar channel distinct from surrounding electric activity so that RMCC is surrounded by >5 ripple bars on either side without sequential activation, (3) presence of fractionated signals/double potentials, (4) channel with a higher bipolar voltage bordered by lower voltage (voltage gradient) using manual adjustment, (5) onset of signals late within the QRS and spanning beyond the QRS. After ablation, the entire process should be repeated to confirm the absence of conduction in all RMCCs. These criteria may require further adjustment with prospective data assessment.

Limitations

This is a retrospective observational study and therefore functional confirmation of all RMCCs using pacing maneuvers was not available and the correlation of ablation lesions with identified RMCCs and VT recurrence was not a direct analysis. However, the aim of this study was to assess the feasibility of visualizing slow conduction channels within the scar using RM and to find evidence of their functional relevance.

Conclusions

RM enables functional mapping of scar by allowing the simultaneous display of electrogram voltage and timing data. It has enabled us to identify channels of slow conduction within the ischemic scar supporting the VT substrate. Prospective work using RM to guide catheter ablation in ischemic VT will further clarify the clinical importance of these slow-conducting channels.

Sources of Funding

Dr Jamil-Copley was supported by the British Heart Foundation (grant number PG/10/37/28347).

Disclosures

Dr Kanagaratnam and N. Linton have received honoraria from Biosense Webster relating to Ripple Mapping. Imperial College owns the Intellectual Property rights of Ripple Mapping on behalf of Dr Kanagaratnam, N. Linton, and Dr Francis. The other authors report no conflicts.

References

1. de Bakker JM, van Capelle FJ, Janse MJ, Wilde AA, Coronel R, Becker AE, Dingemans KP, van Hemel NM, Hauer RN. Reentry as a cause of ventricular tachycardia in patients with chronic ischemic heart disease: electrophysiologic and anatomic correlation. *Circulation*. 1988;77:589–606.
2. Marchlinski FE, Callans DJ, Gottlieb CD, Zado E. Linear ablation lesions for control of unmappable ventricular tachycardia in patients with ischemic and nonischemic cardiomyopathy. *Circulation*. 2000;101:1288–1296.
3. Stevenson WG, Wilber DJ, Natale A, Jackman WM, Marchlinski FE, Talbert T, Gonzalez MD, Worley SJ, Daoud EG, Hwang C, Schuger C, Bump TE, Jazayeri M, Tomassoni GF, Kopelman HA, Soejima K, Nakagawa H; Multicenter Thermocool VT Ablation Trial Investigators. Irrigated radiofrequency catheter ablation guided by electroanatomic mapping for recurrent ventricular tachycardia after myocardial infarction: the multicenter thermocool ventricular tachycardia ablation trial. *Circulation*. 2008;118:2773–2782. doi: 10.1161/CIRCULATIONAHA.108.788604.
4. Tung R, Mathuria N, Michowitz Y, Yu R, Buch E, Bradfield J, Mandapati R, Wiener I, Boyle N, Shivkumar K. Functional pace-mapping responses for identification of targets for catheter ablation of scar-mediated ventricular tachycardia. *Circ Arrhythm Electrophysiol*. 2012;5:264–272. doi: 10.1161/CIRCEP.111.967976.
5. Di Biase L, Santangeli P, Burkhardt DJ, Bai R, Mohanty P, Carbucicchio C, Dello Russo A, Casella M, Mohanty S, Pump A, Hongo R, Beheiry S, Pelargonio G, Santarelli P, Zucchetti M, Horton R, Sanchez JE, Elayi CS, Lakkireddy D, Tondo C, Natale A. Endo-epicardial homogenization of the scar versus limited substrate ablation for the treatment of electrical storms in patients with ischemic cardiomyopathy. *J Am Coll Cardiol*. 2012;60:132–141. doi: 10.1016/j.jacc.2012.03.044.
6. Della Bella P, Bisceglia C, Tung R. Multielectrode contact mapping to assess scar modification in post-myocardial infarction ventricular tachycardia patients. *Europace*. 2012;14(suppl 2):ii7–ii12. doi: 10.1093/europace/eus213.
7. Della Bella P, Baratto F, Tsiachris D, Trevisi N, Vergara P, Bisceglia C, Petracca F, Carbucicchio C, Benussi S, Maisano F, Alfieri O, Pappalardo F, Zangrillo A, Maccabelli G. Management of ventricular tachycardia in the setting of a dedicated unit for the treatment of complex ventricular arrhythmias: long-term outcome after ablation. *Circulation*. 2013;127:1359–1368.
8. Carbucicchio C, Ahmad Raja N, Di Biase L, Volpe V, Dello Russo A, Trivedi C, Bartoletti S, Zucchetti M, Casella M, Russo E, Santangeli P, Moltrasio M, Tundo F, Fassini G, Natale A, Tondo C. High-density substrate-guided ventricular tachycardia ablation: role of activation mapping in an attempt to improve procedural effectiveness. *Heart Rhythm*. 2013;10:1850–1858. doi: 10.1016/j.hrthm.2013.09.059.
9. Jaïs P, Maury P, Khairy P, Sacher F, Nault I, Komatsu Y, Hocini M, Forclaz A, Jadidi AS, Weerasooryia R, Shah A, Derval N, Cochet H, Knecht S, Miyazaki S, Linton N, Rivard L, Wright M, Wilton SB, Scherr D, Pascale P, Roten L, Pederson M, Bordachar P, Laurent F, Kim SJ, Ritter P, Clementy J, Haïssaguerre M. Elimination of local abnormal ventricular activities: a new end point for substrate modification in patients with scar-related ventricular tachycardia. *Circulation*. 2012;125:2184–2196. doi: 10.1161/CIRCULATIONAHA.111.043216.
10. Vergara P, Trevisi N, Ricco A, Petracca F, Baratto F, Cireddu M, Bisceglia C, Maccabelli G, Della Bella P. Late potentials abolition as an additional technique for reduction of arrhythmia recurrence in scar related ventricular tachycardia ablation. *J Cardiovasc Electrophysiol*. 2012;23:621–627. doi: 10.1111/j.1540-8167.2011.02246.x.
11. Arenal A, del Castillo S, Gonzalez-Torrecilla E, Atienza F, Ortiz M, Jimenez J, Puchol A, García J, Almendral J. Tachycardia-related channel in the scar tissue in patients with sustained monomorphic ventricular tachycardias: influence of the voltage scar definition. *Circulation*. 2004;110:2568–2574. doi: 10.1161/01.CIR.0000145544.35565.47.
12. Hsia HH, Lin D, Sauer WH, Callans DJ, Marchlinski FE. Anatomic characterization of endocardial substrate for hemodynamically stable reentrant ventricular tachycardia: identification of endocardial conducting channels. *Heart Rhythm*. 2006;3:503–512. doi: 10.1016/j.hrthm.2006.01.015.

13. Mountantonakis SE, Park RE, Frankel DS, Hutchinson MD, Dixit S, Cooper J, Callans D, Marchlinski FE, Gerstenfeld EP. Relationship between voltage map "channels" and the location of critical isthmus sites in patients with post-infarction cardiomyopathy and ventricular tachycardia. *J Am Coll Cardiol*. 2013;61:2088–2095. doi: 10.1016/j.jacc.2013.02.031.
14. Linton NW, Koa-Wing M, Francis DP, Kojodjojo P, Lim PB, Salukhe TV, Whinnett Z, Davies DW, Peters NS, O'Neill MD, Kanagaratnam P. Cardiac ripple mapping: a novel three-dimensional visualization method for use with electroanatomic mapping of cardiac arrhythmias. *Heart Rhythm*. 2009;6:1754–1762. doi: 10.1016/j.hrthm.2009.08.038.
15. Jamil-Copley S, Linton N, Koa-Wing M, Kojodjojo P, Lim PB, Malcolme-Lawes L, Whinnett Z, Wright I, Davies W, Peters N, Francis DP, Kanagaratnam P. Application of ripple mapping with an electroanatomic mapping system for diagnosis of atrial tachycardias. *J Cardiovasc Electrophysiol*. 2013;24:1361–1369. doi: 10.1111/jce.12259.
16. Stevenson WG, Khan H, Sager P, Saxon LA, Middlekauff HR, Natterson PD, Wiener I. Identification of reentry circuit sites during catheter mapping and radiofrequency ablation of ventricular tachycardia late after myocardial infarction. *Circulation*. 1993;88(4 Pt 1):1647–1670.
17. Stevenson WG, Friedman PL, Sager PT, Saxon LA, Kocovic D, Harada T, Wiener I, Khan H. Exploring postinfarction reentrant ventricular tachycardia with entrainment mapping. *J Am Coll Cardiol*. 1997;29:1180–1189.
18. Biermann M, Shenasa M, Borggrefe M, Hindricks G, Haverkamp W, Breithardt G. The interpretation of cardiac electrograms. In: Shenasa M, Borggrefe M, Breithardt G, eds. *Cardiac Mapping*. Mount Kisco, NY: Futura Publishing. 1993:11–34.
19. Anderson KP, Walker R, Fuller M, Dustman T, Ershler PR, Lux RL. Criteria for local myocardial electrical activation: effects of electrogram characteristics. *IEEE Trans Biomed Eng*. 1993;40:169–181. doi: 10.1109/10.212057.
20. Kienzle MG, Miller J, Falcone RA, Harken A, Josephson ME. Intraoperative endocardial mapping during sinus rhythm: relationship to site of origin of ventricular tachycardia. *Circulation*. 1984;70:957–965.

Circulation
Arrhythmia and Electrophysiology

Application of Ripple Mapping to Visualize Slow Conduction Channels Within the Infarct-Related Left Ventricular Scar

Shahnaz Jamil-Copley, Pasquale Vergara, Corrado Carbucicchio, Nick Linton, Michael Koa-Wing, Vishal Luther, Darrel P. Francis, Nicholas S. Peters, David Wyn Davies, Claudio Tondo, Paolo Della Bella and Prapa Kanagaratnam

Circ Arrhythm Electrophysiol. 2015;8:76-86; originally published online December 19, 2014;
doi: 10.1161/CIRCEP.114.001827
Circulation: Arrhythmia and Electrophysiology is published by the American Heart Association, 7272 Greenville Avenue, Dallas, TX 75231

Print ISSN: 1941-3149. Online ISSN: 1941-3084

SUPPLEMENTAL MATERIAL

Video Legends

Video 1: Higher voltage regions (≥1.02mV) are seen in purple and lower voltage regions (≤1mV) in cyan blue. Antero-apical septal scar is evident (≤1.5mV). The maximum ripple bar voltage setting starts at ± 0.94mV and is gradually reduced to 0.2mV. This allows the visualization of electrograms at or above this value as dynamic ripple bars. The color at the tip of the ripple bar is green at zero-point and transitions to red when the voltage reaches the peak positive clipped value, or blue for peak negative clipped value.

Sequential dynamic ripple bar propagation is analysed within the scar during sinus rhythm. Ripple bar activation is seen entering the scar from the septum with late activity at the lateral scar border which confirms the presence of a continuous channel of ripple bar propagation across the mid/lower anterior wall. The surface bipolar scar voltage is gradually reduced as described in the methods section of the manuscript (which can be seen in the bottom right hand of the screen). Specific attention is paid to the correlation between ripple bar propagation and surface voltage gradient channels highlighted during voltage adjustment. Portions of the ripple bar conduction channel overlap the voltage gradient channel which is defined as a Ripple Mapping Conduction Channel (RMCC).

Electrograms corresponding to the identified RMCCs are selected and highlighted to the left of the screen confirming a propagation channel as seen by the ripple bar activity. A 12/12 pacemap match was achieved within the antero-septal portion of this channel with ablation successfully terminating the clinical VT adjacent to this location (see manuscript Fig.1).

Video 2: Higher voltage regions (≥1.5mV) are seen in purple and lower voltage regions (≤1.48mV) in cyan blue. Anterior wall scar involving the septum and lateral walls is evident (≤1.5mV). The maximum ripple bar voltage is set at ± 0.68mV which allows the visualization of electrograms at or above this value as dynamic ripple bars. The color at the tip of the ripple bar is green at zero-point and transitions to red when the voltage reaches the peak positive clipped value, or blue for peak negative clipped value.

Sequential dynamic ripple bar propagation can be seen from the septum across the anterior wall towards the lateral border. The surface bipolar scar voltage is gradually reduced as described in the methods section of the manuscript (which can be seen in the bottom right corner of the screen) and highlights a voltage gradient channel corresponding with the ripple bar propagation channel. This is defined a Ripple Mapping Conduction Channel (RMCC). Electrograms corresponding to the RMCC are selected and highlighted to the left of the screen confirming a propagation channel as seen by the ripple bar activity. The bipolar surface voltage is reduced further to fully highlight the connections of the channel at the scar border zones. Mid-diastolic electrograms were seen within this channel during VT which terminated during ablation at this location (see manuscript Fig.2).

Video 3: Higher voltage regions are seen in purple and lower voltage regions in cyan blue. Apical scar is evident (≤1.5mV). The maximum ripple bar voltage is set at ±0.56mV and is gradually reduced to 0.45mV (bottom right of screen) which allows the visualization of electrograms at or above this value as dynamic ripple bars. The color at the tip of the ripple bar is green at zero-point and transitions to red when the voltage reaches the peak positive clipped value, or blue for peak negative clipped value.

The top right hand panel in the screen displays the surface QRS with the latest inscription allowing appreciation of late activity. Sequential propagation of ripple bars is seen entering the scar from base to apex. A row of ripple bar double potentials can be appreciated visually without any voltage adjustments or electrogram selection however for the readers' appreciation the electrograms have been selected and highlighted.

Video 4: Higher voltage regions (≥1.5mV) are seen in purple and lower voltage regions (≤0.42mV) in cyan blue. Inferior wall scar is evident in cyan blue (≤1.5mV). The maximum ripple bar voltage is set at ±0.14mV (bottom right of screen) which allows the visualization of electrograms at or above this value as dynamic ripple bars. The color at the tip of the ripple bar is green at zero-point and transitions to red when the voltage reaches the peak positive clipped value, or blue for peak negative clipped value.

The top right hand panel in the screen displays the surface QRS with the latest inscription allowing appreciation of late activity. Sequential ripple bar activation is seen crossing the scar from the lateral border towards the septum.

1. Several channels of sequential conduction can be appreciated within the scar
2. These channels consist of electrograms with relatively higher voltage amplitude (i.e. larger bars) compared with surrounding bars in the scarred myocardium.
3. The conducting channels are slower compared to the surrounding normal myocardium (>1.5mV) seen in purple.
4. The channels consist of abnormal electrograms (ripple bars are continually moving up and down throughout activation=fractionation) which occur late (activation starting late in the QRS or after the end of the QRS (seen in the top right corner of the screen). We have selected

electrograms to highlight to the readers what we have described above although all of the aforementioned points can be appreciated without any voltage adjustment or electrogram selection.